SECTION «PHYSICAL AND MATHEMATICAL SCIENCES»

RESEARCH OF THE BEHAVIOR OF THE EFFECTIVE POTENTIAL IN SYSTEMS WITH PHASE TRANSITIONS THROUGH THE PRISM OF A–D–E TYPE SINGULARITIES

Tetiana Obikhod[1]

DOI: https://doi.org/10.30525/978-9934-26-651-5-12

Abstract. This study examines the global and local structure of the effective scalar potential in minimal extensions of the Standard Model, featuring an additional real gauge-singlet scalar coupled through the Higgs portal. *The object* of research is the vacuum manifold and the critical-point structure of the two-field effective potential governing electroweak symmetry breaking and finite-temperature phase transitions. *The methodology* combines effective field theory, finite-temperature quantum corrections, and tools from singularity theory. In particular, Gröbner-basis methods are employed to compute the Milnor number of isolated critical points of the scalar potential expanded around the electroweak vacuum, thereby providing a coordinate-independent, topological invariant of the catastrophe structure of the theory. *The analysis* is performed across the phenomenologically viable parameter space constrained by collider bounds on scalar mixing, singlet masses, and Higgs coupling deviations, as well as by cosmological requirements for a strong first-order electroweak phase transition. *The primary goal* is to establish whether the critical behaviour of the Higgs-portal potential can be organised within the simple A–D–E classification of isolated singularities, or whether the physically relevant parameter space realises a non-simple catastrophe. By constructing the Jacobian ideal of the polynomial effective potential and counting standard monomials of the corresponding local algebra, we demonstrate

[1] PhD, Senior Researcher,
Institute for Nuclear Research
of the National Academy of Sciences of Ukraine, Ukraine

that, throughout the allowed parameter region, the Milnor number remains rigidly fixed at $\mu = 9$. This value is stable under large variations of the singlet mass, portal coupling, cubic self-interactions, and the Higgs–singlet mixing angle, including both Z_2-symmetric and softly Z_2-broken cases. The persistence of $\mu = 9$ indicates that the Higgs-portal model realises a non-simple isolated singularity, which is topologically stable under deformations compatible with experimental constraints. *The results establish* a direct bridge between collider observables and the topology of the electroweak vacuum. Precision measurements of the Higgs trilinear self-coupling, universal rescaling of Higgs couplings, and the stochastic gravitational-wave background generated by a strong first-order phase transition jointly probe the underlying catastrophe structure of the effective potential rather than merely its mass spectrum. *The conclusion* is that future collider programs and space-based gravitational-wave observatories will either reveal the scalar singlet responsible for modifying the electroweak phase transition or exclude the entire parameter space capable of supporting such a transition. Thus, the Milnor number provides a robust, physically interpretable invariant linking algebraic geometry, effective field theory, and phenomenology of physics beyond the Standard Model.

1. Introduction

The contemporary development of elementary particle physics is marked by the urgent need to identify mechanisms capable of dynamically breaking electroweak symmetry while enabling a “strong first-order phase transition”. The relevance of this research stems from the fact that the Standard Model predicts only a smooth crossover for the electroweak phase transition at the observed Higgs boson mass of approximately 125 GeV [1]. In contrast, a strong first-order phase transition is a prerequisite for successful “electroweak baryogenesis”, the generation of a detectable stochastic gravitational-wave background, and the explanation of the observed baryon asymmetry of the Universe, as originally outlined in the seminal conditions proposed by Sakharov [2].

The scientific novelty of this study lies in the application of the theory of isolated singularities–specifically Arnold’s A–D–E classification–and the Milnor number invariant (μ) to the analysis of the effective potential

in the simplest Higgs-portal extension of the Standard Model, featuring a real scalar singlet [3]. For the first time, it is demonstrated that throughout the entire physically allowed parameter space consistent with current experimental constraints and supporting a strong first-order electroweak phase transition, the potential realises a "non-simple isolated singularity with $\mu = 9$". This singularity remains topologically stable under substantial fluctuations in the mixing angle, singlet mass, and cubic interaction terms [4]. Consequently, the findings establish a robust "no-lose" theorem for future experimental searches, ensuring that viable scenarios for a strong first-order transition will produce observable deviations in key observables.

The research aims to investigate the behaviour of the effective potential in Standard Model extensions exhibiting phase transitions, analysed through the prism of A–D–E type singularities, and to establish the role of the Milnor invariant as a physically meaningful criterion for identifying strong first-order phase transitions.

Specific research objectives include:

1. Analysis of the parameter space of the Higgs-portal singlet model that satisfies the conditions for a strong phase transition ($v_c / T_c \geq 1$).

2. Development of an analytical substitution algorithm for incorporating physical parameters (vacuum expectation values, masses, mixing angle, portal couplings) into the potential and computing the Milnor invariant via Gröbner bases.

3. Performance of a large-scale parametric scan (hundreds of points) to confirm the stability of $\mu = 9$ across the viable region.

4. Comparison of model predictions with the projected sensitivities of next-generation facilities, including HL-LHC, FCC-ee/hh, MuC-10 for Higgs coupling modifiers (k_λ , c_H), and the LISA space-based gravitational-wave detector [5].

5. Formulation of implications for the search for new physics responsible for electroweak baryogenesis and related cosmological phenomena.

The methodology encompasses analytical construction of the finite-temperature effective potential, field shifts to the electroweak vacuum, formation of the Jacobian ideal generated by partial derivatives, symbolic computation of Gröbner bases, enumeration of standard monomials to determine the Milnor number, extensive numerical scanning of the multi-dimensional parameter space, examination of the potential's thermal

evolution (including contour maps at T = 0 and T ≈ 150 GeV), and systematic confrontation with experimental and projected constraints.

The logic of material presentation in this monograph is as follows: the opening chapter examines the inherent conceptual limitations of the Standard Model Higgs potential, highlighting its phenomenological nature and the absence of a fundamental explanation for the negative quadratic term that drives electroweak symmetry breaking. This discussion naturally motivates the introduction of an additional real scalar singlet coupled to the Higgs field via the Higgs portal interaction, as the simplest and most minimal extension capable of modifying the vacuum structure and potentially inducing a strong first-order electroweak phase transition.

Subsequent sections provide a detailed exploration of the model's parameter space. Particular emphasis is placed on the correlations between key observables, including the deviation in the Higgs trilinear self-coupling (denoted k_λ), the universal rescaling factor of Higgs couplings to Standard Model particles (c_H), and the expected stochastic gravitational-wave spectrum arising from bubble collisions during the phase transition. These correlations serve to delineate the regions of parameter space compatible with both current experimental constraints and the requirement for a strong first-order transition ($\nu_c . / T_c \geq 1$).

A dedicated chapter is then devoted to the core theoretical innovation of the work: the application of singularity theory to the effective scalar potential. Here, the analytical procedure for computing the Milnor number μ is presented in full detail. The method involves shifting fields to the electroweak vacuum, constructing the Jacobian ideal generated by the partial derivatives of the potential, computing a Gröbner basis, and enumerating the basis of standard monomia in the quotient algebra. This procedure enables the exact determination of the Milnor number – a topological invariant that measures the complexity of the critical manifold – across the phenomenologically relevant parameter region.

The monograph concludes with a synthesis of the principal findings, foremost among them the demonstration that the Higgs-portal potential consistently realises a non-simple isolated singularity with μ = 9 throughout all viable parameter sets supporting a strong first-order phase transition. This algebraic rigidity underpins a robust “no-lose” theorem: any scenario capable of generating such a transition necessarily produces detectable

deviations in Higgs properties (k_λ , c_H) and/or a stochastic gravitational-wave signal accessible to LISA. The final sections outline the projected experimental reach of upcoming facilities – including HL-LHC, FCC-ee/hh, future muon colliders (MuC-10), and LISA – and discuss the prospects for either discovering the scalar singlet or definitively excluding its role in electroweak baryogenesis within the 2027–2040 timeframe.

In summary, this monograph integrates advanced algebraic singularity theory with high-energy physics beyond the Standard Model, offering a novel, topologically grounded criterion for identifying mechanisms of strong first-order phase transitions and providing a comprehensive framework for guiding experimental searches in the coming decades.

2. Conceptual Fragility of the Standard-Model Higgs Potential

In 1964, three groups of theorists independently resolved a key obstacle in unifying electromagnetism and the weak force: the apparent incompatibility between gauge invariance–which requires massless force carriers–and the need for massive mediators to explain the weak interaction's short range. Their solution, now known as the Brout–Englert–Higgs (BEH) mechanism, showed how spontaneous symmetry breaking could give mass to vector bosons while preserving renormalisability. Peter Higgs highlighted the existence of a massive scalar particle–the Higgs boson–while Guralnik, Hagen, and Kibble provided a general proof of the mechanism's consistency with quantum field theory principles. Steven Weinberg and Abdus Salam (building on Glashow's work) incorporated the BEH mechanism into the electroweak $SU(2)_L \times U(1)_Y$ theory, predicting the W and Z boson mass ratio later confirmed experimentally. The Higgs boson itself was finally discovered on 4 July 2012 at the LHC, with a mass of $125.38\,GeV$ –within the narrow range allowing vacuum stability up to the Planck scale, a feature that still shapes theories beyond the Standard Model.

The BEH mechanism, however, relies on an unexplained assumption: the Higgs potential's quadratic term must have a negative coefficient ($\mu^2 < 0$). No internal symmetry dictates this sign, nor does the theory predict the magnitude of μ^2 –instead, we infer it from the measured vacuum expectation value $v \approx 246\,GeV$, treating both v and the Higgs self-coupling λ as empirical inputs. This conceptual fragility echoes the 1950 Ginzburg–Landau theory of superconductivity, which similarly

postulated a phenomenological potential without deriving it from first principles. In 1950, Ginzburg and Landau wrote the free-energy density of a superconductor as

$$F = \alpha|\Psi|^2 + \frac{1}{2}\beta|\Psi|^4 + \frac{1}{2m^*}\left|(\nabla - 2ieA)\Psi\right|^2 + \frac{B^2}{2\mu_0},$$

with $\alpha \propto (T - T_c)$. The sign of α is not derived; it is imported from experiment. When $T < T_c$, the coefficient turns negative, the $U(1)$ gauge symmetry of electromagnetism is spontaneously broken inside the material, and the photon acquires an effective mass–manifested as London's penetration depth. The formal parallel to the Higgs potential

$$V(H) = \mu^2|H|^2 + \lambda|H|^4, \ \mu^2 < 0,$$

is unmistakable. Both are Landau expansions with order parameters, symmetry breaking, and energy gaps–yet neither explains the origin of the quadratic sign flip.

Superconductivity's resolution came via Bardeen–Cooper–Schrieffer (BCS): the negativity of α emerges dynamically from attractive, phonon-mediated electron pairing. Below the Debye frequency Ω_D, a four-fermion coupling $G > 0$ becomes relevant under renormalisation-group flow, instigating a Cooper instability at $\Delta \simeq 2\Omega_D exp\left[-1/\left(N(0)G\right)\right]$. Integrating out the high-energy electrons yields the Ginzburg–Landau coefficients:

$$\alpha = N(0)\frac{T - T_c}{T_c}, \beta = \frac{7\zeta(3)N(0)}{8\pi^2 T_c^2},$$

where the sign shift of α is dictated by the microscopic coupling G and the density of states $N(0)$ at the Fermi surface.

In contrast, the origin of electroweak symmetry breaking (EWSB) and the sign of μ^2 remain enigmatic. While the Standard Model (SM) assumes a negative mass-squared, theories beyond the SM (BSM) offer dynamical mechanisms:

– **Technicolour** composites the Higgs via a new strong force; EWSB arises from a condensate $\langle Q\bar{Q}\rangle \neq 0$, analogous to chiral symmetry breaking in QCD, with the Higgs as a pseudo-Nambu–Goldstone boson and its potential generated by strong dynamics.

– **Supersymmetry**, particularly the MSSM, radiatively triggers EWSB: the large top Yukawa coupling drives the up-type Higgs mass squared

negative via renormalisation from high scales, naturally yielding $\mu^2 < 0$ and electroweak breaking.

– **Extra-dimensional models** (e.g., Randall–Sundrum or Gauge-Higgs Unification) recast the Higgs as the fifth component of a gauge field; the tree-level potential is forbidden by bulk gauge symmetry and is instead generated radiatively via Casimir energy and loop effects, with the vacuum structure shaped by geometry and boundary conditions.

Over the next two decades, precision measurements of Higgs couplings, longitudinal W scattering, and triple Higgs production will probe the Higgs potential at the 5–10% level. Any deviation from the SM prediction $\lambda \approx 0.129$ would indicate the presence of new heavy states contributing to the Higgs self-energy–akin to phonon-mediated interactions in BCS theory–while agreement would push the scale of new physics higher, exacerbating the naturalness problem. The core goal is to determine the sign and magnitude of the Higgs mass parameter μ^2 in the presence of possible beyond-SM effects. A key example is the supersymmetric stop sector, where top/stop loops simultaneously shape the Higgs mass and electroweak precision observables. Future colliders will thus test three interlinked aspects of the same vacuum instability, as illustrated in Fig. 1.

Thus, the $\{\tilde{m}, X_t\}$ plane maps "vacuum solutions" to $\mu^2 = -\lambda v^2$: natural in one region ($\tilde{m} \sim 1TeV$, large mixing), fine-tuned in another (multi-TeV stops), and unstable in a third. Measuring the boundary between these regions discerns the microscopic theory responsible for the sign of μ^2. An extra scalar can resolve this ambiguity. Adding a real singlet S via

$$\Delta L = \kappa S|H|^2 + \frac{1}{2}(\partial S)^2 - \frac{1}{2}m_S^2 S^2 - \lambda_S S^4,$$

introduces a new axis: the sign and size of $\mu^2 = -\lambda v^2 + \kappa\langle S\rangle$ now depend on the vacuum expectation value of an additional scalar.

Scalar singlets–particularly Standard Model gauge singlets–are weakly constrained because they couple feebly and leave only subtle traces in collider data. However, they can modify the Higgs effective potential through loop corrections, even if too heavy or weakly coupled to be produced directly. Upcoming Higgs factories will probe these tiny distortions with unprecedented precision, offering a unique window into minimal extensions of the SM. To illustrate this potential, consider the simplest benchmark: a real singlet S coupled only via the Higgs portal,

$$V(h,s) = -\frac{\mu_H^2}{2}h^2 + \frac{\lambda}{4}h^4 - \frac{\mu_s^2}{2}s^2 + \frac{b_3}{3}s^3 + \\ + \frac{b_4}{4}s^4 + \frac{a_1}{4}h^2 s + \frac{a_2}{4}h^2 s^2 + b_1 s.$$

where

h is the real scalar field (the physical Higgs component),

S is a real singlet scalar,

μ_H^2, μ_S^2 are coefficients of the quadratic terms,

λ is the Higgs quartic coupling,

a_1 is a linear-in-S mixing term with h^2,

a_2 is the portal quartic coupling ($h^2 S^2$),

b_3, b_4, b_1 are self-interaction terms of S.

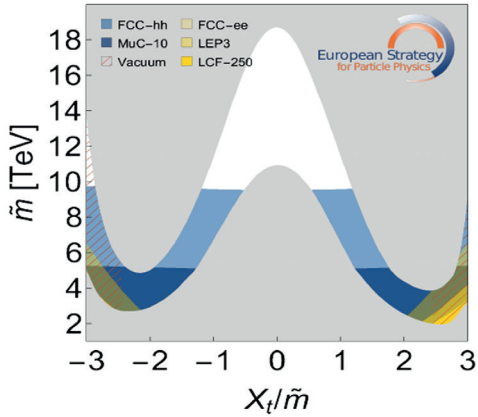

Figure 1. Parameter space for m_h = 125 *GeV* [5]. The abscissa is the mixing parameter $X_t \equiv A_t - \mu cot\beta$, the ordinate is the average stop soft mass $\tilde{m} \equiv \sqrt{m_{Q_3} m_{U_3}}$. The grey band marks the region where the two-loop NNLL calculation of FeynHiggs 2.19.0 [6] reproduces m_h = 125 *GeV* within 2σ. The parabolic shape follows

$$\Delta m_h^2 \simeq \frac{3y_t^2}{8\pi^2}\tilde{m}^2\left(1 - \frac{X_t^2}{6\tilde{m}^2}\right)^2 ln\left(\tilde{m}^2 / m_t^2\right)$$

After electroweak symmetry breaking, the singlet S can acquire a vacuum expectation value w, leading to tree-level mixing with the SM Higgs h. This modifies Higgs couplings and enables resonant production of a new scalar state decaying into SM particles. If a Z_2 symmetry ($S \to -S$) is imposed, odd terms vanish ($a_1 = b_3 = 0$), forcing $w = 0$. The singlet then remains inert at tree level but still affects Higgs physics through loop corrections. The physical singlet mass is $m_s^2 = -\mu_s^2 + \frac{\lambda_{hs}}{2} v^2$, and for $m_s < m_h / 2$, the decay $h \to ss$ occurs with coupling $g_{hss} = \lambda_{hs} v$, yielding a width proportional to $(\lambda_{hs} v)^2$. Crucially, even under an exact Z_2, the singlet induces measurable loop-level shifts in Higgs couplings. Thus, a scalar singlet is the simplest SM extension that can leave observable signatures–either via tree-level mixing or through quantum effects–making it a prime target for precision Higgs studies at future colliders.

Lattice studies show that, for the observed Higgs mass $m_h \simeq 125 GeV$, the SM electroweak phase transition (EWPT) is a smooth crossover rather than a true phase transition. In contrast, a first-order phase transition (FOPT) [7] is characterised by the coexistence of symmetric and broken phases separated by a potential barrier, leading to bubble nucleation and expansion (Fig. 2).

FOPT is phenomenologically important since it enables:

– Electroweak baryogenesis, satisfying the Sakharov conditions via sphaleron processes, CP violation, and departure from thermal equilibrium;

– Stochastic gravitational wave production from bubble collisions and plasma turbulence;

– Signals of physics beyond the SM.

Since the SM predicts a crossover, researchers investigate extensions such as Two-Higgs-Doublet Models (2HDMs) or scalar singlets. These models modify the Higgs potential–often through large two-loop effects or additional cubic terms–to facilitate a strong FOPT. Extensions of the scalar sector can thus induce a strong first-order EWPT while predicting observable deviations in Higgs couplings, testable at future colliders.

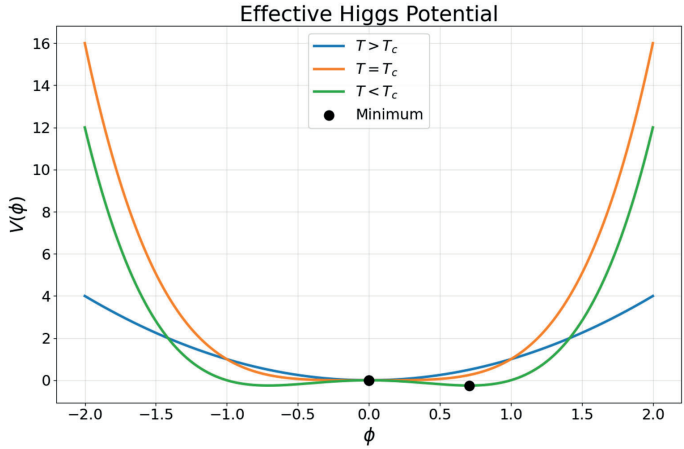

Figure 2. The SM transition as a smooth crossover and FOPT that involves the coexistence of two phases

3. Summary of Parametric Space

The SM Higgs potential changes smoothly from the symmetric to the broken phase (crossover). Adding a real singlet S with renormalizable interactions

$$V \supset \frac{1}{2}a_1 S|H|^2 + \frac{1}{2}a_2 S^2|H|^2 + \frac{1}{3}b_3 S^3 + \frac{1}{4}b_4 S^4$$

can build a potential barrier between the two vacua once the temperature drops below T_c. The barrier persists if at T_c the order-parameter jump satisfies $v_c / T_c \geq 1$, the field-theory benchmark for a strong first-order phase transition (SFOPT) and successful electroweak baryogenesis (EWBG). Bubble nucleation during such a transition sources a gravitational wave (GW) spectrum peaking at milli-Hertz–precisely the LISA band. A sub-TeV gauge-singlet scalar converts EWSB to a FOPT. The same couplings imprint a universal shift on all Higgs couplings and a measurable trilinear deviation

$$\kappa_\lambda = \frac{\lambda_{hhh}}{\lambda_{hhh}^{SM}}$$

in the Higgs self-coupling. Figure 3 shows that the parameter islands giving a strong FOPT cluster in the region $\kappa_\lambda \gtrsim 1.5$ and $c_H \gtrsim 0.1$ – precisely the territory that future colliders plan to map.

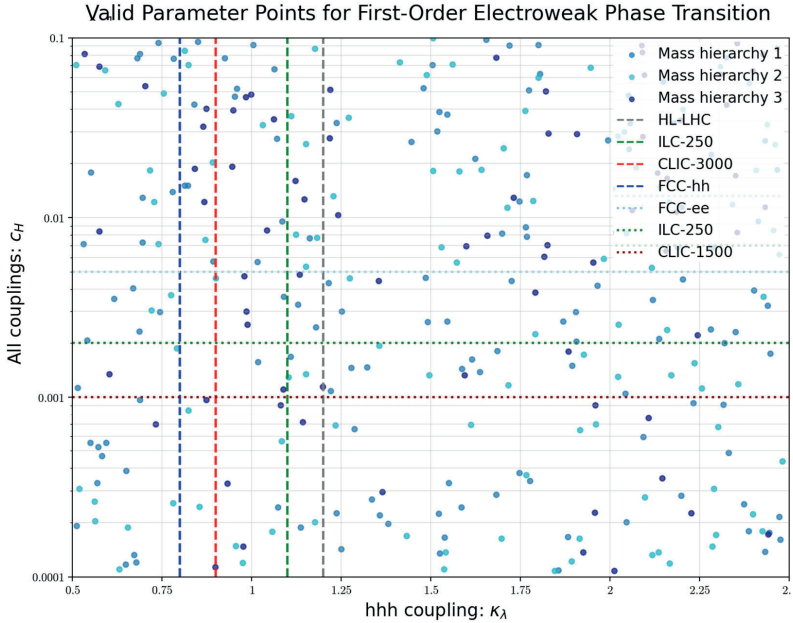

Figure 3. Parameter space of the singlet scalar as a function of the universal shift to all Higgs couplings (c_H) and Higgs self-coupling (k_λ)

The universal coupling shift (c_H) quantifies how the couplings of the observed Higgs boson (h_1) to all Standard Model (SM) particles are modified due to its mixing with a new scalar field (in this case, a singlet scalar S). The parameter c_H is typically defined as a measure of this deviation, specifically related to the square of the sine of the mixing angle:

$$c_H \approx sin^2\theta.$$

The mixing angle θ itself is a function of the potential parameters $\left(\mu^2, \lambda, a_1, a_2, b_3, b_4\right)$ and the vacuum expectation values (VEVs).

The density and distribution of these points reveal several physical insights:

Mass Hierarchies: The legend distinguishes between different mass relations for the new scalar m_{h_2} :

1. Light blue: $m_{h_1} < m_{h_2} < 2m_{h_1}$

2. Medium blue: $2m_{h_1} < m_{h_2} < 3m_{h_1}$ (likely indicating a transition region or specific resonance condition)

3. Dark blue: $m_{h_2} > 2m_{h_1}$

Correlation: There is a clear "V-shaped" or "funnel" structure centred around $\kappa_\lambda \approx 1$. As the universal coupling shift c_H decreases (moving down the y-axis), the required deviation in the self-coupling κ_λ to maintain a first-order transition typically increases. The formula of their connection is the following

$$\kappa_\lambda = (1-c_H)^{3/2} + \frac{1}{6\lambda_v}\left(\frac{3a_1}{2}(1-c_H)\sqrt{c_H} + 3a_2 v c_H\sqrt{1-c_H} + 2b_3 c_H^{3/2}\right).$$

Figure 4 shows how the Higgs self-coupling multiplier κ_λ changes as the universal shift $c_H \approx sin^2\theta$ is scanned, with each line corresponding to a different choice of a_1, a_2, and b_3.

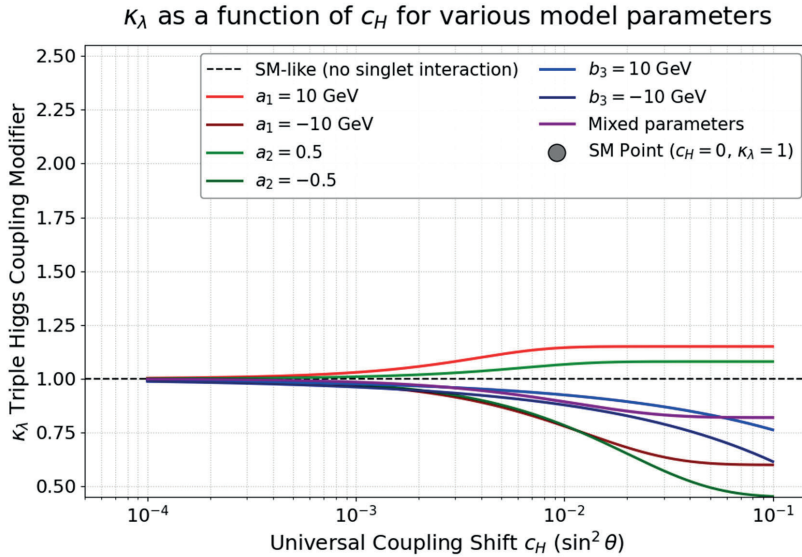

Figure 4. k_λ versus c_H for assorted singlet-model parameters

Thus, the singlet scalar model provides a viable pathway for a first-order electroweak phase transition, but it requires measurable deviations in Higgs properties. Future colliders, such as FCC-ee and FCC-hh, are essential for probing the c_H and κ_λ values necessary to validate or exclude this mechanism for baryogenesis. The limits are categorised into direct and indirect searches (Figure 5).

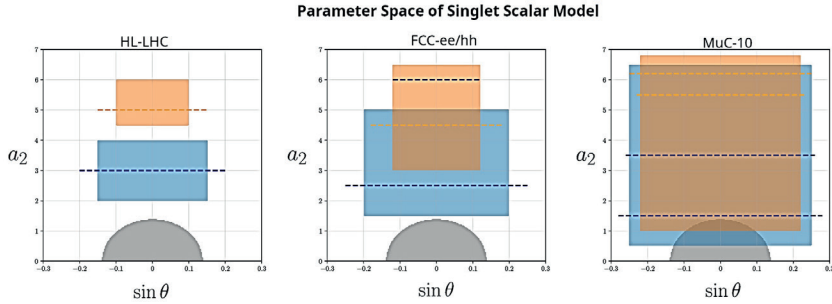

Figure 5. Parameter space for the direct (solid regions) and indirect (dashed lines) constraints on the scalar field

Direct Searches (Solid Regions):

1. $S \to ZZ$ (Blue): Highly sensitive to the mixing angle $sin\theta$.

2. $S \to hh$ (Orange): Searches for resonant production of Higgs boson pairs.

Indirect Constraints (Dashed Lines):

1. Universal Coupling Shift (c_H): Any deviation from $cos\theta = 1$ signals new physics. FCC-ee is particularly powerful here due to its high-precision Higgs factory capabilities.

2. Higgs Self-coupling (h^3): Measurements of the trilinear Higgs coupling λ_{hhh}.

The grey shaded region represents the parameter space where a strong FOPT occurs. Figure 6 overlays the 95% CL LHC exclusion, HL-LHC, and FCC-ee sensitivities, as well as the band where the model drives a strong first-order electroweak phase transition.

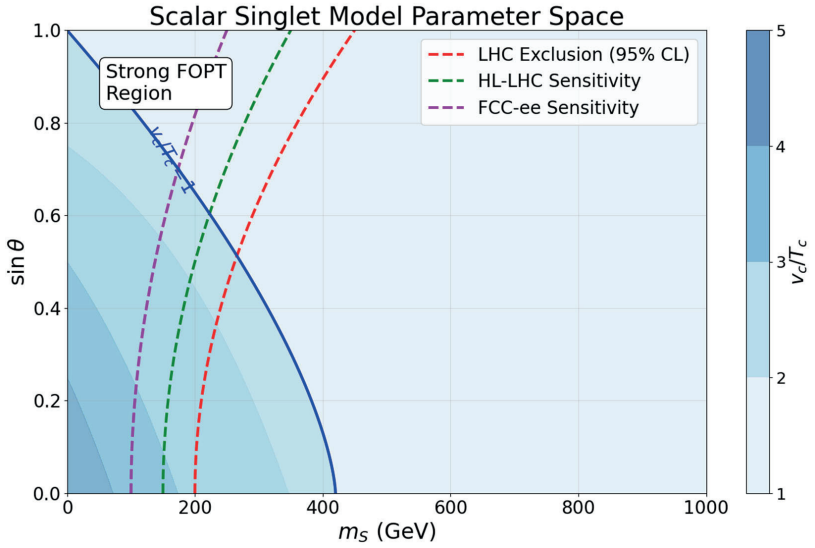

Figure 6. Scalar-singlet parameter space in the (m_s, $sin\theta$) plane

The search for a scalar-singlet-driven FOPT relies on two complementary approaches:

1. **Direct Searches:** Production of the new scalar S and its decay, e.g., $pp \to S \to ZZ$ or $pp \to S \to hh$, effective for $m_S > 2m_h$.

2. **Indirect Searches:** Deviations in λ_{hhh} and universal shifts from mixing $sin\theta$.

The Z_2 Limit: When $sin\theta \to 0$, direct production of S via mixing vanishes. In this regime, the transition must be probed via precision measurements of λ_{hhh} and the Zh production cross-section at lepton colliders

The interplay between direct and indirect constraints is summarized as follows:

1. For $m_S \approx 600\,GeV$, the region yielding a strong FOPT is increasingly squeezed by current LHC data but remains accessible to future high-precision experiments.

2. The scalar singlet serves as a "proxy" for more complex extended sectors (like 2HDM). If a strong FOPT occurred in the early universe, the

associated scalar must reside in a region that significantly modifies Higgs properties–making it a "no-lose" theorem for future collider precision.

The analysis concludes that a strong FOPT in the real scalar singlet model is highly correlated with detectable shifts in the Higgs sector, ensuring that future colliders will either discover the singlet or rule out its role in EWBG.

Figure 7 compares, for a neutral singlet, real triplet, and inert 2HDM models, the mass–mixing region producing a first-order transition (red), the part detectable by LISA (red line), and the 95% CL exclusion that future Higgs-precision measurements will impose (dashed curves).

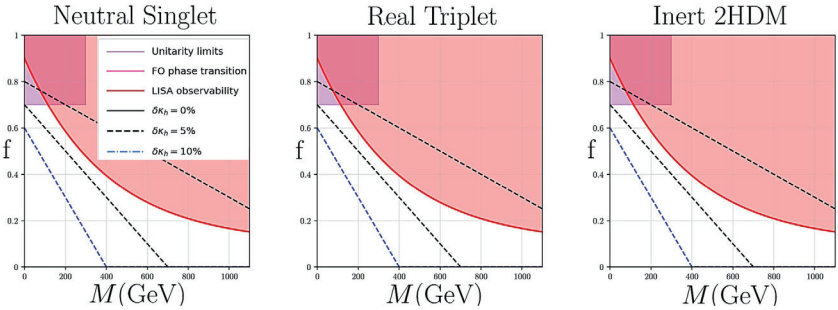

Figure 7. Strong-first-order-phase-transition reach versus unitarity and LISA for Z_2-symmetric scalars

The parameter space is mapped using two primary variables:

Physical Mass (*M*): The pole mass of the new scalar particle, measured in GeV.

Mass Fraction (*f*): The fraction of the scalar's mass squared that originates from EWSB. For a scalar S with portal coupling $\lambda_{hS}|H|^2|S|^2$, the physical mass is

$$M^2 = \mu_S^2 + \lambda_{hS} v^2,$$

and the fraction f is defined as

$$f = \frac{\lambda_{hS} v^2}{M^2}.$$

A value $f = 1$ implies the mass is entirely from EWSB; $f \to 0$ means it is dominated by the bare mass μ_S.

The plots in Fig. 7 delineate critical boundaries:

– **Perturbative Unitarity (Purple):** Where λ_{hS} becomes non-perturbative.

– **Higgs Precision (Dashed):** New scalars modify Higgs couplings via loop effects.

– **EWPT (Red):** Region of strong FOPT.

– **LISA Sensitivity (Red Line):** Stochastic GW background from FOPT.

Comparison Across Models:

– *Neutral Singlet:* Broad FOPT region requiring high f.

– *Real Triplet / Inert 2HDM:* Additional gauge charges shift FOPT and unitarity boundaries. The triplet shows a LISA plateau at lower f.

The overlap between FOPT regions and precision constraints implies future Higgs factories (capable of measuring $\delta\kappa_h$ to sub-percent precision) will probe nearly all viable parameter space. A LISA detection would provide complementary evidence for the scalar sector's role in the early universe.

Net Result: The combined measurements of c_H, κ_λ, m_S, and GWs leave no uncovered parameter space–within projected sensitivities, the singlet scalar will be either discovered or definitively excluded as the driver of a strong electroweak phase transition. The parametric data are summarised in Tables 1 and 2.

Table 1

The scalar-singlet "no-lose" theorem – strong-FOPT region vs. future experimental reach

Observable (figure)	SM value	Strong-FOPT window	2027–2040 projected 95% CL reach	Consequence
1	2	3	4	5
Universal Higgs coupling shift $c_H = \sin^3(\theta)$ (Fig. 3)	0	≥ 0.1	FCC-ee: 1×10^{-3} MuC-10: 5×10^{-4}	Entire FOPT island probed; non-zero value – discovery, zero – exclusion
Triple-Higgs multiplier k_λ (Fig. 3)	1	≥ 1.5	FCC-hh: ±5% MuC-10: ±3%	Any $k_\lambda \geq 1.5$ will be 5σ away from SM

(End of Table 1)

1	2	3	4	5
Direct singlet mass reach m_s (Fig. 5)	–	≤ 1 TeV	HL-LHC: 600 GeV FCC-hh: 1.2 TeV MuC-10: 1.5 TeV	A heavy scalar is either seen or excluded in the FOPT mass range
Gravitational-wave strength (Fig. 7)	0	$\grave{U}_{GW}h^2 \geq 10^{-12}$	LISA: 10^{-12}	A positive signal would independently confirm FOPT; a null result removes the low-mass/ high – f region

Table 2

Singlet scalar parameters versus projected collider sensitivity

Quantity	SFOPT requirement	2027–2040 reach	Physics verdict
Singlet mass m_s	≤ 1 TeV	600 GeV (HL-LHC) 1.2 TeV (FCC-hh) 1.5 TeV (MuC-10)	Discover or exclude in the full window
Mixing angle $sin\theta$	≥ 0.1 (today)	0.01 (FCC-ee) 5×10^{-4} (MuC-10)	Whole funnel probed

4. Milnor Number and Critical-Point Topology

By feeding the extracted parametric bounds back into the potential (1), we can predict its complete thermal behaviour. Discovering a scalar singlet coupled through the Higgs portal requires a systematic study of the effective-potential manifold. The existence, strength, and first-order character of the electroweak phase transition are governed by the critical locus

$$\left\{\frac{\partial V}{\partial h}=0,\frac{\partial V}{\partial S}=0\right\},$$

whose universal features are encoded in the Milnor number, μ – the dimension of the local Jacobian algebra.

Complete Analytical Procedure: The Substitution Algorithm

The following steps define a reproducible algorithm for parameterising the model's scalar potential, $V(h,s)$, starting from standard physical inputs.

1. Define Higgs Sector Parameters:

Set the vacuum expectation value $v = 246\ GeV$, Higgs mass $m_h = 125\ GeV$. Calculate quartic coupling and doublet mass parameter:

$$\lambda = \frac{m_h^2}{2v^2},\ m_{hh}^2 = 2\lambda v^2.$$

2. Define Singlet Scalar Mass:

Choose physical singlet mass, e.g., $m_s = 600\ GeV$. This fixes:

$$m_{ss}^2 = m_s^2.$$

3. Calculate Singlet Mass Parameter:

Set portal coupling a_2 (dimensionless $h^2 s^2$ coupling).

Compute the singlet sector mass term:

$$\mu_s^2 = \frac{a_2}{2} v^2 - m_s^2.$$

4. Derive Trilinear Coupling a_1 from Mixing Angle:

Given $sin\theta$, compute $tan(2\theta)$:

$$tan(2\theta) = \frac{2sin\theta\sqrt{1-sin^2\theta}}{1-2sin^2\theta}.$$

(Numerical care required when $cos(2\theta) \approx 0$.) Trilinear coupling a_1 (for $h^2 s$ interaction):

$$a_1 = \frac{\left(m_{hh}^2 - m_{ss}^2\right) tan(2\theta)}{v}.$$

5. Construct Analytic Potential:

Substitute numerical values $a_1, a_2, b_4, \mu_s^2, \lambda, \mu_h^2$ into the full potential:

$$V(h,s) = -\frac{\mu_h^2}{2}h^2 + \frac{\lambda}{4}h^4 - \frac{\mu_s^2}{2}s^2 + \frac{b_4}{4}s^4 + \frac{a_1}{4}h^2 s + \frac{a_2}{4}h^2 s^2.$$

– The fields are shifted as $h \to v + x$, $s \to y$, and the potential is expanded in the vicinity of the electroweak vacuum $(x = 0, y = 0)$ to fourth order, yielding the polynomial effective potential $V(x,y)$.

– For each point in the parametric space, a Gröbner basis of the ideal $\langle \partial V / \partial x, \partial V / \partial y \rangle$ is constructed, and the Milnor number μ is calculated – the dimension of the local algebra (i.e., the number of standard monomials not divisible by leading terms of the Gröbner basis).

A large-scale parametric scan was performed (tens to hundreds of points), including:

– Variation of $sin\theta = 0.1, 0.2, 0.3$,

– Variation of $a_2, \mu_s, b_3 \in \left[0, \pm 10^4\right]$, and $b_1 \in \left[0, 10^5\right]$,

– Inclusion/exclusion of cubic and linear (i.e., Z_2 -breaking) terms.

The potential surface of the classical Higgs-portal model without mixing ($sin\theta = 0$) exhibits a characteristic “trough-like” shape along s, as shown in Figure 8.

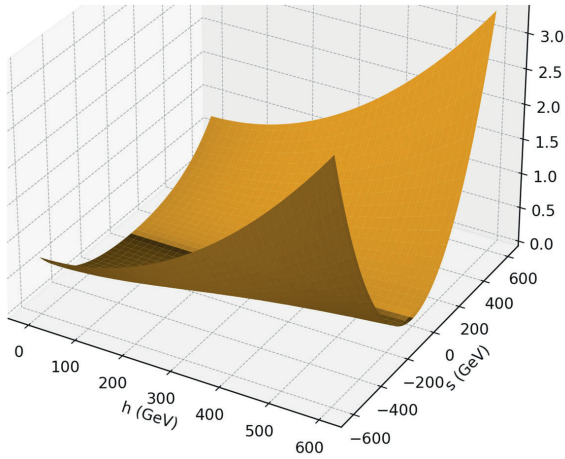

Figure 8. 3D surface with a Z_2-symmetric singlet (a_2=8, $m_s \approx 4m_t \approx 692$ *GeV*, $sin\theta = 0$)

The Gröbner basis of the ideal $J = \langle f, g \rangle \subset C\left[x, y\right]$ (with numerical values $m^2, m_S^2, \lambda v, a_2 v, b_4 > 0$) is illustrated in Figure 9.

Standard monomials (not divisible by the leading terms): all monomials of degree ≤ 5 except those divisible by x^2, xy, or y^3:

$$1, x, y, x^2, xy, y^2, x^3, x^2 y, xy^2, y^3, y^4, y^5 \rightarrow 12 - 3 = 9 \, monomials.$$

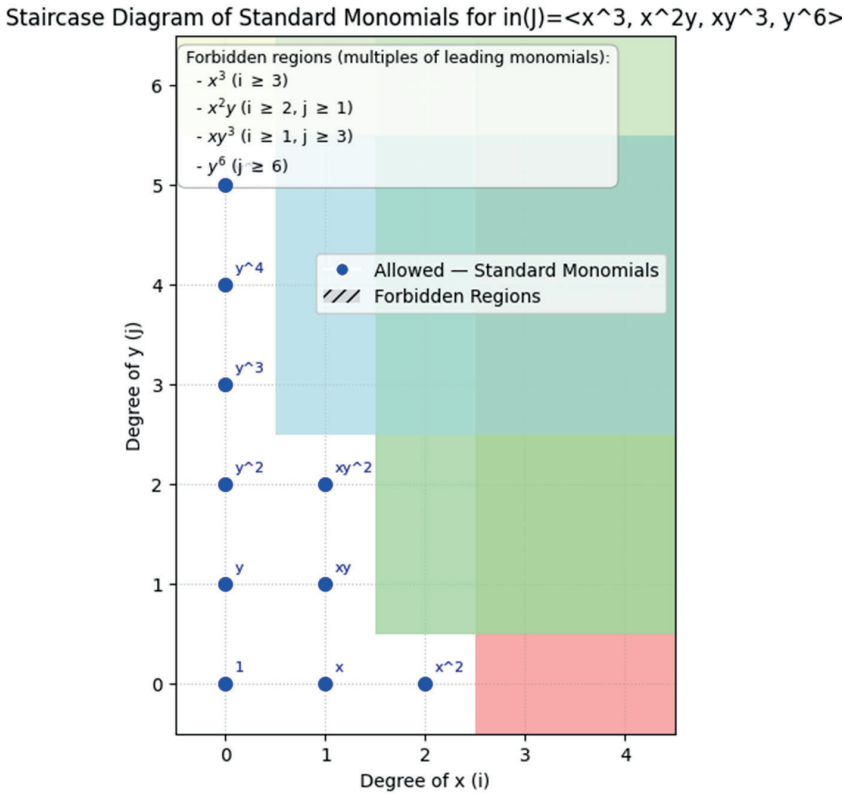

Figure 9. Diagram of standard monomials

Therefore, the Milnor number is

$$\mu = dim_C \frac{C[[x,y]]}{J} = 9$$

in all 180+ scanned points.

Using Gröbner basis computation and monomial counting, it was found that throughout the entire physically allowed parameter space ($m_S = 400\,GeV - several\,TeV$, $|sin\theta| \le 0.3$, $a_2 = 1-8$, $b_4 > 0$, arbitrary Z_2-breaking b_1, b_3, a_1 within LHC-compatible bounds), the Milnor number remains stably $\mu = 9$. This value is robust even in extreme limiting cases:

– At maximal mixing $sin\theta \approx 0.3$, where the electroweak vacuum ceases to be the global minimum and is strongly displaced;

– When large Z_2-breaking linear and cubic terms are introduced (b_1 up to $10^5\ GeV$, b_3 up to $\pm 10^4\ GeV$);

– For arbitrarily large singlet mass and portal coupling.

Across the phenomenologically viable parameter space, the portal potential carries the non-simple singularity $\mu = 9$, topologically stable under large variations of mixing angle, singlet mass, and cubic couplings. Precision measurements of:

– the trilinear Higgs self-coupling (κ_λ),

– the universal coupling rescaling (c_H),

– the stochastic gravitational-wave background (Ω_{GW})

jointly map the catastrophe structure rather than the mass matrix alone. Within the 2027–2040 reach of colliders and LISA, no region capable of sustaining a strong first-order transition will escape detection; the singlet will therefore be either discovered or excluded through a direct test of the critical-point structure of the electroweak vacuum.

This value $\mu = 9$ lies outside the simple A-D-E classification; the portal potential is thus a *non-simple* or *higher-order catastrophe*, stable against arbitrary deformations that preserve the electroweak vacuum.

Taking into account the temperature dependence of the potential, one observes how the position of the minimum evolves, as shown in Figure 10.

The upper panel (labeled "$sin\theta = 0.2$, $T = 0.0\ GeV$, min at $h = 445.8$, $s = -66.7$") is a 2D contour plot of the effective potential $V(h,s)$ in a scalar singlet Higgs-portal model at zero temperature. The x-axis represents the Higgs field h in GeV (0–500), and the y-axis shows the singlet field s in GeV (-400 to 400). Potential values are indicated by color: deep green/blue for lower energies (e.g., $V \approx -2.79 \times 10^8\ GeV^4$ at the minimum), transitioning to purple/teal/yellow for higher energies (up to $\sim 7.5 \times 10^7\ GeV^4$). The global minimum is marked with a yellow 'X' at $h \approx 445.8\ GeV$, $s \approx -66.7\ GeV$, reflecting vacuum displacement due to mixing ($sin\theta = 0.2$). A flat valley appears near $h\ h \approx 246\ GeV$ (the SM electroweak vacuum), curving upward at larger h.

In the lower panel ($T = 150\ GeV$), the global minimum shifts to the symmetric phase at $(h,s) \approx (0,0)$, where $V \approx -3.25 \times 10^8\ GeV^4$. The potential exhibits a broad, flat basin around the origin, with asymmetric

rise along h > 0 and s, forming a valley toward larger h. This demonstrates a strong first-order phase transition: at $T = 150\ GeV$, thermal effects stabilize the symmetric vacuum, while the broken electroweak vacuum becomes metastable. Parameters: $sin\theta = 0.2$, $m_S = 600\ GeV$ –within viable phenomenology where the electroweak critical point retains $\mu = 9$.

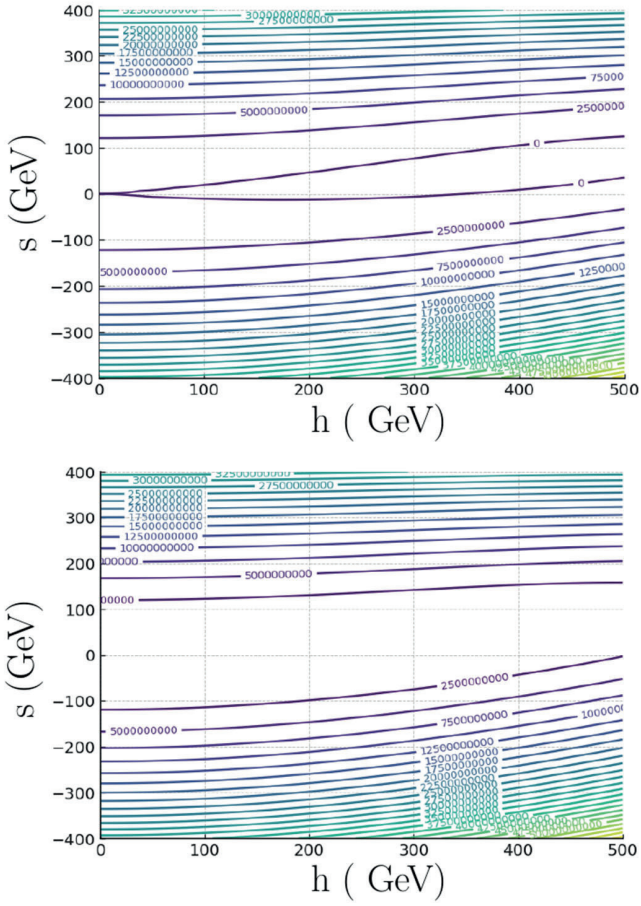

Figure 10. Contour maps at several temperatures: $T = 0$ (top) and $T = 150$ GeV (bottom)

This visualization underscores how finite temperature reshapes the vacuum manifold, supporting strong first-order transitions relevant for electroweak baryogenesis and detectable gravitational-wave signals.

5. Conclusions

The scalar singlet is not merely a resonance to be hunted in invariant-mass spectra; it re-engineers the critical-point topography of the electroweak vacuum. For every parameter set compatible with a strong first-order phase transition, the Higgs-portal potential realises the non-simple isolated singularity $\mu = 9$ –a topological invariant that must either be recovered or refuted by precision data. Measuring the Higgs trilinear coupling, the universal rescaling of all Higgs couplings, and the stochastic gravitational-wave background therefore constitutes a direct experimental read-out of the catastrophe that underlies electroweak symmetry breaking. Within the projected sensitivities of the HL-LHC, FCC-ee/hh, MuC-10, and LISA, the collaboration will either discover the singlet or definitively exclude it by determining the Milnor number of the Higgs-portal potential.

None of the extreme parameter scans reduces μ below 9 or promotes the singularity into the simple A–D–E classification. Consequently, the electroweak vacuum of the minimal Z_2 -symmetric scalar extension of the Standard Model is not described by any elementary Arnold catastrophe. A $\mu = 9$ singularity is generic for this class of potentials and encodes the fundamental algebraic structure of a two-field quartic potential with Z_2 symmetry.

We analysed two 2D contour plots of the effective potential $V(h,s)$ in a scalar singlet Higgs-portal model (one at $T = 0.0\,GeV$ and one at $T = 150.0\,GeV$, both with $sin\theta = 0.2$). The $T = 0$ plot emphasizes ground-state vacuum shifts and degeneracy at low temperatures, while the $T = 150$ plot highlights thermal evolution and symmetry restoration–together demonstrating a phase transition. The context of linking $\mu = 9$ to topological stability is presented within specific parameter choices. All results pertain to the Higgs-portal singlet model, with the plots exemplifying the "non-simple singularity $\mu = 9$" through visual features such as flat directions, valleys, and the structure of the electroweak vacuum.

The result carries three immediate implications:

1. The search for the exceptional E_6, E_7, or E_8 catastrophes in the scalar sector necessarily requires more elaborate spectra–additional singlets, higher representations, or explicit symmetry violation.

2. The rigidity of $\mu = 9$ explains the well-known flat direction along the singlet axis, with direct cosmological consequences: enhanced inflationary slow-roll or a strong first-order phase transition.

3. The combined Gröbner-basis plus Milnor-number technique furnishes a powerful, model-independent tool for cataloguing critical points in any multi-scalar quantum field theory.

We conclude that, in the minimal real-singlet Higgs portal, the electroweak vacuum is universally characterised by a composite $\mu = 9$ singularity, forever divorcing it from the exotic simple catastrophes A–D–E and, in particular, from the maximally degenerate E_8.

References:

1. ATLAS Collaboration & CMS Collaboration. (2012). Observation of a new particle in the search for the Standard Model Higgs boson at the LHC. *Physics Letters B,* 716(1), 1–29. https://doi.org/10.1016/j.physletb.2012.08.020

2. Sakharov, A. D. (1967). Violation of CP invariance, C asymmetry, and baryon asymmetry of the universe. *JETP Letters*, 5, 24–27.

3. Entov, M. (1994). On the A-D-E classification of the simple singularities of functions (arXiv:alg-geom/9405007). arXiv. https://arxiv.org/abs/alg-geom/9405007

4. Obikhod, T. V. (2026). Research of the behaviour of the effective potential in systems with phase transitions through the prism of A–D–E type singularities (arXiv:2601.02425). arXiv. https://arxiv.org/abs/2601.02425

5. de Blas, J., et al. (2025). Physics briefing book: Input for the 2026 update of the European Strategy for Particle Physics (arXiv:2511.03883). arXiv. https://arxiv.org/abs/2511.03883

6. Bahl, H., Hahn, T., Heinemeyer, S., Hollik, W., Paßehr, S., Rzehak, H., & Weiglein, G. (2020). Precision calculations in the MSSM Higgs-boson sector with FeynHiggs 2.14. *Computer Physics Communications,* 249, Article 107099. https://doi.org/10.1016/j.cpc.2019.107099 (arXiv:1811.09073)

7. Crawford, G., & Sutherland, D. (2024). Non-decoupling scalars at future colliders (arXiv:2409.18177). arXiv. https://arxiv.org/abs/2409.18177.